JGR Planets

RESEARCH ARTICLE
10.1029/2020JE006397

Groundwater Flow to Gale Crater in an Episodically Warm Climate

Mark Baum[1] and **Robin Wordsworth**[1,2]

[1]Department of Earth and Planetary Science, Harvard University, Cambridge, MA, USA, [2]Paulson School of Engineering and Applied Sciences, Harvard University, Cambridge, MA, USA

Key Points:
- Tens of thousands of years are likely required to generate significant groundwater flow to Gale Crater with a thawing crust
- Surface water would likely be the dominant source for Gale lakes at the beginning of a warm episode
- Deep aquifers may have played a role later on if complete thaw occurred beneath Gale

Correspondence to:
M. Baum,
markbaum@g.harvard.edu

Citation:
Baum, M., & Wordsworth, R. (2020). Groundwater flow to Gale Crater in an episodically warm climate. *Journal of Geophysical Research: Planets*, *125*, e2020JE006397. https://doi.org/10.1029/2020JE006397

Received 27 JAN 2020
Accepted 18 JUL 2020
Accepted article online 23 JUL 2020

Abstract Orbiter and rover data have revealed a complex and intermittent hydrological history in Gale Crater on Mars, where habitable environments appear to have endured for at least thousands of years. The intermittency may be the result of a dominantly cold climate punctuated by geologically brief periods of warmth and active hydrology. However, the time required to establish an integrated hydrological cycle in a warming climate is difficult to ascertain and has not been thoroughly investigated. Here we model the transient evolution of groundwater flow and subsurface temperature, the slowest evolving components of the hydrological cycle, during a warm departure from cold conditions. We find that tens of thousands of years are likely required before groundwater could be a meaningful source for large lakes in Gale. With highly favorable conditions, primarily high permeability, significant flow might develop in thousands of years. This implies that surface water dominates during the beginning of a warm phase. Annual mean surface temperatures in Gale below 290 K would likely leave the nearby highlands frozen at the surface. In that case, deep aquifers beneath a highlands permafrost layer could deliver water to Gale, where low temperatures would have reduced evaporation.

Plain Language Summary Satellite imagery and data from the National Aeronautics and Space Administration (NASA)'s *Curiosity* rover indicate that Gale Crater, on Mars, hosted large lakes more than 3 billion yr ago. The climate during this period is not well understood but may have been mostly frozen, only occasionally warming up to the point where lakes could form. If so, warm periods must have been long enough to thaw frozen sources of water and supply the lakes. The slowest thawing source is groundwater. We simulate the thawing and flow of groundwater in the region surrounding Gale to understand whether it could have been a significant source for lakes during a warm climate period. We find that it could only be significant with the most generous assumptions about flow speed and aquifer recharge. Even with generous assumptions, tens of thousands of years are required to thaw enough groundwater to have an impact on large lakes. After long enough, though, the ground would thaw entirely, possibly enabling a higher rate of groundwater delivery.

1. Introduction

The nature of the early Martian climate is a long-standing puzzle. It has implications for the search for our understanding of the origins of life and planetary climate evolution (Haberle et al., 2017; Wordsworth, 2016). More than three billion years ago, Mars hosted conditions much warmer and hydrologically active than the frozen deserts on its surface today. Its ancient crust preserves evidence of large-scale hydrological activity with liquid water at the surface (Fassett & Head, 2008; Grotzinger et al., 2015; Hynek et al., 2010; Williams et al., 2013) and its mineralogy implies widespread aqueous alteration (Ehlmann & Edwards, 2014). However, an array of climate models, from one-dimensional radiative calculations to complex global climate models, demonstrate that sustaining a warm climate on early Mars with a faint young sun requires more than a $CO_2 - H_2O$ greenhouse, even a very thick one (Kasting, 1991; Ramirez et al., 2014; Steakley et al., 2019; Wordsworth et al., 2010, 2013, 2017; Urata & Toon, 2013).

Many ideas have emerged to explain the gulf between climate physics and surface observations. Large meteorite impacts (Segura, 2002; Steakley et al., 2019); volcanic SO_2 emission (Halevy et al., 2007; Halevy & Head, 2014); CO_2 and/or H_2O clouds (Forget, 1997; Urata & Toon, 2013); and periodic warming by diurnal, seasonal, and orbital cycles (Palumbo et al., 2018; Wordsworth et al., 2013) have all been explored. All these mechanisms, however, have limited long-term warming potential (Forget et al., 2013; Kerber et al.,

2015; Ramirez et al., 2014; Ramirez & Craddock, 2018; Wordsworth, 2016). Limit cycles are an intriguing possibility (Batalha et al., 2016; Hayworth et al., 2020) and reducing greenhouse gas emission is under investigation (Chassefire et al., 2016; Haberle et al., 2019; Ramirez et al., 2014; Sagan, 1977; Wordsworth & Pierrehumbert 2013; Wordsworth et al., 2017), but these mechanisms may only generate occasional warming. Given the temporal limitations of all these warming mechanisms and the magnitude of warming required under a faint young Sun, the early Martian climate may have been mostly cold, episodically warmed by, perhaps, a combination of overlapping forcings. In this scenario, evidence of active hydrology on the Martian surface is the result of warm climate states enduring for only a small fraction of the roughly 1 billion yr we consider "early Mars."

Gale crater, home to the *Curiosity* rover, is currently the most closely examined place on the surface of Mars. Intense study of stratigraphy, morphology, and geochemistry in the crater has documented large ancient lakes and fluvial systems, clear evidence of conditions warm enough to support active hydrology, at least regionally and briefly. Closely studied sedimentary deposits beneath Mount Sharp are thought to have required 10^3 to 10^7 yr to form (Fukushi et al., 2019; Grotzinger et al., 2014, 2015; Stack et al., 2019), a wide range. The full thickness of sediment traversed by the rover extends the total duration of lacustrine activity (Fedo et al., 2018), but analyses of the Murray formation suggest significant variability in climate and lake level (Rapin, 2019; Stein et al., 2018; Thomas et al., 2019). After these sediments were deposited, lacustrine activity was probably mostly absent as aeolian material filled the crater and was subsequently excavated, forming Mount Sharp. Later, multiple lake stands that participated in a "sustained and full hydrologic cycle" but with varying sources that appear to have switched on and off suddenly. The duration of these later lakes is also unknown, but the estimated cumulative time to form the observed sedimentary structures is 10^4 to 10^5 yr (Palucis et al., 2016). As a whole, investigation of Gale has revealed a complex history with perhaps many separate periods of lacustrine activity. The cumulative duration of lakes at all stages may only be a small fraction of the $>10^8$ yr available during the Late Noachian and Hesperian periods.

Intermittent lakes in Gale crater would be compatible with a primarily cold climate punctuated by periods of hydrological activity. However, the time required to develop a well-integrated hydrological cycle in a warming climate is difficult to constrain. This timescale is critical to interpreting the climatic implications of Gale's geologic history. If lakes were only episodically sustained in Gale, the time required to activate sources of lake water must be similar to or less than the time needed to build the observed fluvio-lacustrine structures.

Here we investigate how one branch of the hydrological cycle, groundwater flow, may have contributed to lakes in Gale crater after a transition from cold to warm surface temperatures. Gale's deep crater floor and location directly at the base of Mars's hemispheric dichotomy make it a very likely destination for topographically driven groundwater flow. Multiple lines of evidence suggest groundwater activity in the crater at different times in its history (Frydenvang et al., 2017; Rampe et al., 2017; Palucis et al., 2016; Siebach & Grotzinger, 2014; Thomas et al., 2019; Yen et al., 2017). Hurowitz et al. (2017) interpret mineralogical relationships in the sediment beneath Mount Sharp as evidence of redox stratified lakes with groundwater-derived solute input. Fukushi et al. (2019) also discuss how redox conditions within Gale sediments could be generated by interactions with upwelling groundwater. Groundwater flow and heat transfer are much slower processes than precipitation and runoff. Their long timescales determine the minimum time required to develop a full hydrological cycle, which includes subsurface flow.

Prior work includes integrated hydrological modeling of the region surrounding Gale, including surface processes, to fit lake levels and infer climatic conditions (Horvath & Andrews-Hanna, 2017). Such an integrated approach yields important insight into Gale hydrology under a warm, steady-state climate with a fully thawed crust. However, as we show later, the time required to thaw the crust from a cold equilibrium state is likely tens of thousands of years or more, especially for the high-elevation terrain south of Gale where surface temperatures would be relatively low. This amount of time is a significant fraction of the estimated maximum lake lifetime of about 10^5 yr (Palucis et al., 2016). If lakes in Gale existed during geologically brief periods of warmth, the crust was likely out of thermal equilibrium for a significant portion of their existence and maybe their entire existence.

Here we investigate the effect of a transiently warm climate on groundwater delivery to lakes in Gale and its implications for the inferred climate history. In section 2 we detail our numerical model and choices of physical parameters. In section 3 we explain the simulations performed with the model. In section 4 we

show simulated groundwater fluxes and crustal temperatures. Finally, in section 5 we interpret the results as part of the water budget for Gale lakes, compare with prior work, and discuss the role of deep aquifers with elevation-dependent surface temperature.

2. Model

We use a numerical model of groundwater flow in a thawing crust that is designed to capture the major features of the physical scenario in a robust manner. The model includes one-dimensional, horizontal, unconfined groundwater flow using the Boussinesq equation for unsteady flow (Bear, 1972). Horizontal groundwater flow occurs between the water table and the bottom of the aquifer. Here the aquifer's bottom is the depth where the crust is frozen. The flow rate is determined by the gradient of the water table, depth-dependent hydraulic properties (permeability and porosity), and temperature-dependent viscosity. The governing groundwater equation is

$$n(h)\frac{\partial h}{\partial t} = \frac{\partial}{\partial x}\left(\int_{z_b}^{h} \frac{k(z)\rho_w g}{\mu[T(z)]}\,dz\right) + S_h; \tag{1}$$

where $n(h)$ is the porosity at the water table h, t is time, x is the horizontal dimension, z_b is the bottom of the aquifer (the freezing point), $k(z)$ is the depth-dependent permeability, ρ_w is water's density, g is the gravitational acceleration, $\mu[T(z)]$ is the temperature-dependent viscosity (where the temperature is also depth dependent), and S_h is a source/sink term for aquifer recharge from surface infiltration with units of meters per second. The porosity and permeability functions are exponential with depth,

$$n(d) = n_0 e^{-d/\gamma_n} \quad \text{and} \quad k(d) = k_0 e^{-d/\gamma_k}; \tag{2}$$

where d is the depth below the surface. The uncertainty associated with the porosity and permeability is large, but the general exponential form is expected from Earth analogy and theoretical consideration of the impact fractured Martian crust (Clifford & Parker, 2001; Hanna, 2005; Horvath & Andrews-Hanna, 2017; Rae et al., 2019). To evaluate the importance of these parameters, we span wide ranges of values (Table 1). Variation over the porosity range 0.1-0.4 had little effect on the results, so we use $n_0 = 0.2$ for all trials.

We use an empirical function of water's viscosity appropriate for the temperature range considered (Demming, 2002),

$$\mu(T) = 2.4 \times 10^{-5} \times 10^{248/(T - 140)}. \tag{3}$$

The viscosity only varies by a factor of about 2 over the range 273-300 K. This should have a small effect on flow rates, but it is easy to include in the model and is well understood for water. Solutes also have an effect on water's viscosity, but this effect is normally much smaller (Demming, 2002).

For the temperature field in the crust, we model vertical heat transfer with independent temperature columns, so that the surface temperature may vary spatially. This quasi-two-dimensional approach, uncoupled in the horizontal dimension, is appropriate for the very high aspect ratio of the model domain. Gale Crater is 150 km wide and our simulations are focused on the top 1 km of crust. Heat conduction is governed by the heat equation,

$$\rho_r c \frac{\partial T}{\partial z} = \frac{\partial}{\partial z}\left(\alpha \frac{\partial T}{\partial z}\right); \tag{4}$$

where ρ_r is the bulk density, c is the heat capacity, T is the temperature, z is the vertical dimension, and α is the thermal conductivity. We choose thermal conductivity values based on prior studies of Martian subsurface hydrology (Clifford, 1993; Clifford & Parker, 2001). The latent heat of fusion is incorporated with the apparent heat capacity method (Hu & Argyropoulos, 1996), where temperature cells have elevated heat capacities over a small temperature interval near the freezing point, requiring an extra thermal energy input equivalent to the latent heat. Surface temperatures are elevation dependent according to lapse rates spanning the range between an approximate dry adiabat ($g/c_p \approx 4.5$ K/km) and the average lapse rate in GCM simulations of Mars with a 1 bar CO_2 atmosphere and a large ocean (about 2.5 K/km) (Forget et al., 2013;

Table 1
Values of Key Model Parameters

Parameter	Description	Range/value	Units
k_0	surface permeability	10^{-14} to 10^{-11}	m^2
γ_k	exponential permeability decay length	500-2,500	m
n_0	surface porosity	0.2	m^3/m^3
γ_n	exponential porosity decay length	2,500	m
α_r	rock thermal conductivity	1-6	W/m·K
S_h	groundwater recharge	0-max[a]	m/s
T_{si}	initial surface temperature at the bottom of Gale	220	K
T_{sf}	warmed surface temperature at the bottom of Gale	275-295	K
Γ	lapse rate	2.5-4.5	K/km
Q_g	geothermal heat flux	40	mW/m^2

[a]Max indicates that the water table is kept exactly at the surface.

Wordsworth, 2016). Diurnal and seasonal variation in surface temperature is neglected because variation on those time scales only affects the top few meters. The geothermal heat flux, which constitutes the lower thermal boundary condition of the model, is taken to be 40 mW/m^2, a rough estimate for the Hesperian period on Mars (Hauck, 2002). We ignore the advection of heat, which is negligible for slow groundwater flow nearly perpendicular to the thermal gradient.

We use idealized topography along a north-south transect running through Gale (Figure 1). Because of Gale's location at the base of the hemispheric dichotomy, long-range groundwater flow would be topographically driven down the dichotomy. We create a topographic profile capturing the dichotomy, the full depth of the crater, and the northern crater wall by fitting functions to different parts of the profile. A sigmoid function captures the dichotomy and a superposed Gaussian function captures the crater, with a flat section to the crater's north. The central mound in Gale is ignored so that the crater's maximum depth is included. The mound could be a groundwater source during warming but it is relatively small compared to the surrounding terrain.

Together, these model components capture the effect of increased thickness of crust available for flow near Gale as surface temperatures change and the freezing point propagates downward. The governing Equations 1 and 4 are integrated with second-order finite volume methods and a second-order Runge-Kutta method. The depth integral in Equation 1 is performed along the temperature discretization between groundwater columns, effectively using the composite midpoint rule. The horizontal (groundwater) grid is nonuniformly spaced, denser in steep and/or curved regions, with 532 cells and minimum cell width of about 200 m. The vertical (thermal) grids are denser near the surface, each having 424 cells and a cell depth at the surface of 30 cm. All trials used 60 million uniform time steps or a temporal resolution of about 3.7 hr.

3. Simulations

First, we use the one-dimensional thermal component of our model to quantify the time required for the crust to thaw after transition from cold to warm surface conditions. Starting with a frozen surface

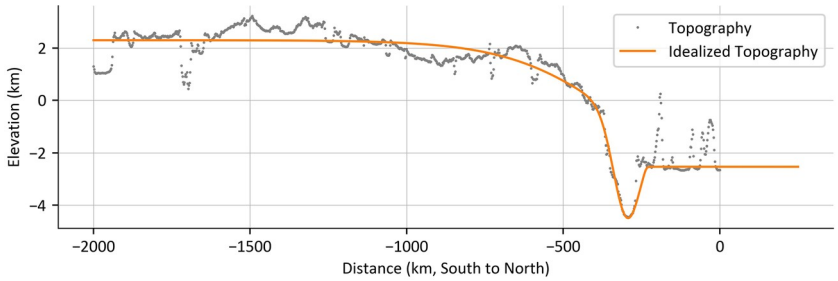

Figure 1. A topographic cross section running south to north through Gale Crater (from MOLA data) and the idealized/smoothed topography used in the model.

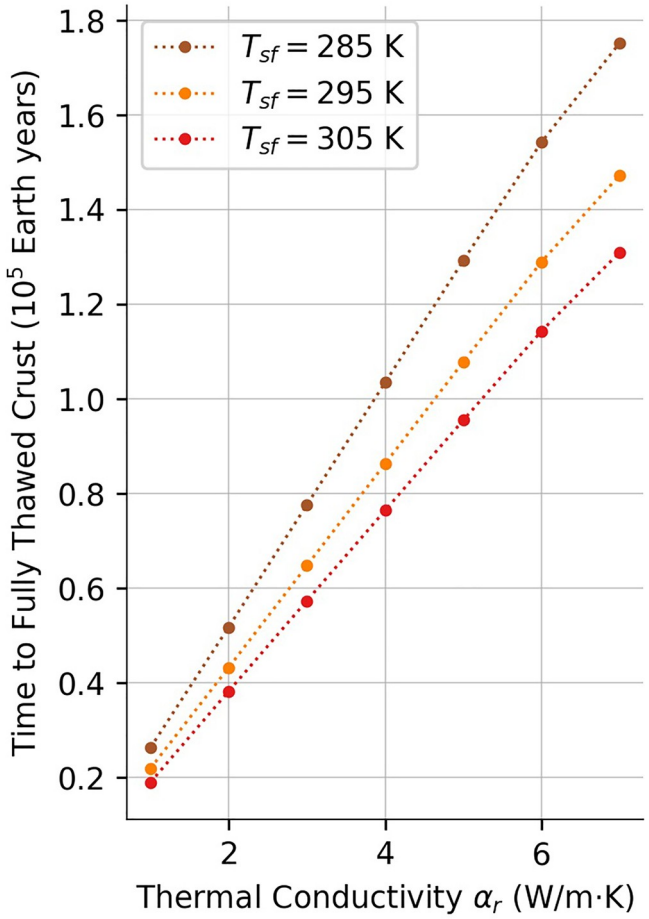

Figure 2. The time required to fully thaw a one-dimensional profile of the crust for a range of thermal conductivities and final surface temperatures. Starting from an initially frozen surface at 220 K and with the crust in geothermal equilibrium, the surface temperature is instantaneously raised to T_{sf}. Porosity is zero for these baseline results, excluding the effect of latent heat, which would only lengthen thaw times. The geothermal heat flux is 40 W/m^2. The time required to thaw the crust for these conditions is at least 2×10^4 yr. Interestingly, higher thermal conductivity *increases* the thaw time because of a shallower initial geothermal gradient. After a transition to a warm climate, the crust is likely to be out of thermal equilibrium for tens of thousands of years, without connection between the surface and any deep aquifers.

temperature at 220 K and a crust in geothermal equilibrium, the surface temperature is instantaneously raised to above freezing. The temperature profile is evolved until it is above freezing everywhere. These relatively simple simulations underscore the motivation for the rest of our simulations using the full model.

Next, we use the full model to examine transient groundwater flow after rapid surface warming. Initially, the surface temperature at the bottom of Gale is set to 220 K, around that predicted by the simulations of Wordsworth et al. (2015) with a baseline CO_2 and H_2O atmosphere. The surface temperature always decreases at higher altitudes according to an atmospheric lapse rate. At the beginning of each simulation, surface temperatures are raised so that the temperature in Gale is either 275, 285, or 295 K. The initial temperature profile of the crust is in equilibrium with a geothermal heat flux of 40 mW/m^2.

The water table is initially at the ground surface, such that the upper layer of the crust is frozen and saturated. Representing the freezing of infiltrating water in a partially saturated, thermally dynamic crust is a considerable modeling challenge, so we focus on the case of an initially saturated crust. By using end members for recharge, we simulate flow rates as the water table drops and the hydraulic gradient shallows, as described below.

Each combination of thermal and hydraulic parameters is run once with maximum recharge, where the water table is exactly at the surface, and once with zero recharge, where the water table responds to flow. Cases with maximum recharge, where the crust is always saturated, represent an upper limit on groundwater flow for the thawing crust. Cases with zero recharge allow feedback between the flow rate and water table height. In reality, some recharge would keep the water table between these end members. For example, even if the crust were initially dry, in 10,000 yr a recharge rate of 1 cm/yr would contribute 500 m to the water table, assuming a porosity of 20%. This is comparable to the depth of thawed crust after the same amount of time. Hence, even for an initially dry crust, the range spanned by zero recharge and maximum recharge is probably a representative range after the first several thousand years of simulation. The maximum recharge cases give a firm upper limit on groundwater flow rates for a given thermal state.

The duration of all model runs is 25,000 Earth years. This is not a suggestion that lakes only persisted in Gale for that length of time, but a choice based on the time required to completely thaw the crust under Gale. For some parameter combinations, the crust beneath Gale is ice free after roughly that length of time, as suggested by Figure 2. At this point, the surface may be hydraulically connected to deeper parts of the crust. We discuss the potential impact of this connection later, but the model is not designed for this complication.

4. Results

Figure 2 shows the time required to thaw a one-dimensional profile of crust, starting from an initially frozen surface. For these results only, we ignore latent heat to estimate minimum thaw times. For the entire range of thermal conductivities considered, more than 2×10^4 yr are required to thaw the frozen upper layer and connect the surface with deeper parts of the crust. For higher conductivities, the time is even longer. These results demonstrate that after a climate transition, the crust is likely to be out of thermal equilibrium for periods of time that may be comparable to the lifetimes of lakes in Gale.

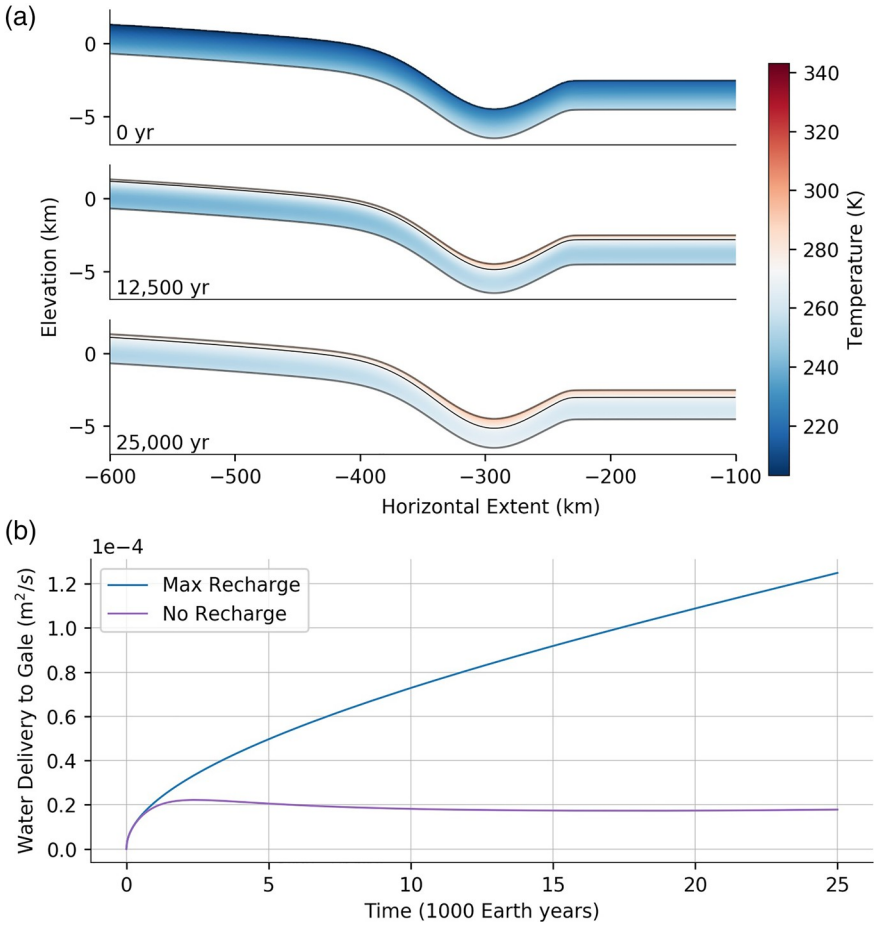

Figure 3. Example results for a trial with $k_0 = 10^{-12}$ m^2, γ_k = 1,000 m, α_r = 2 W/m·K, T_{si} = 220 K, T_{sf} = 295 K, and Γ = 2.5 K/km, integrated for 25,000 Earth years. The top panel (a) shows the temperature field in the model domain at the beginning, middle, and end of the run. The color scale is centered on 273 K and a black contour shows the 273 K isotherm, where present. Parts of the domain far from the crater have been cropped (see Figure 1 for the whole domain). There is significant vertical exaggeration. The bottom panel (b) shows the groundwater flow rate to Gale with maximum recharge and no recharge, for the same thermal parameters. Because the modeled groundwater flow is one-dimensional, the water delivery rate is given in m^2/s.

Figure 3 shows the temperature evolution of the crust for an example model run and groundwater delivery to Gale for the maximum and zero recharge cases. The model domain includes the top 2 km of the crust for all simulations. In each simulation, the thermal gradient near the surface is reversed after the surface temperature is raised and energy is conducted downward, thawing a near-surface layer. This layer becomes available for groundwater flow. As the freezing point propagates downward, the depth of this region grows, increasing the capacity for groundwater flow. For the chosen lapse rate, the surface is above freezing throughout the domain after the temperature in Gale is raised from 220 to 295 K. By the end of the trial, several hundred meters of the crust has been thawed, releasing groundwater to lower elevations. The rate of groundwater delivery steadily increases for the maximum recharge case and is quite stable after a few thousand years for the zero recharge case. Without recharge, the water table is dropping but the flow rate is stabilized by water melted out of the thawing crust as the freezing point drops.

To relate one-dimensional flow rates to the water balance of a lake in Gale, we use a simple mass balance for a closed-basin lake. Assuming the flow occurs perpendicular to a length L with a lake area A and lake evaporation rate E, the groundwater flux F would solely sustain the lake if $FL = EA$. Rearranged, the balancing evaporation rate is $E = FL/A$. This simple conversion was applied to the modeled groundwater delivery for all combinations of the minimum and maximum values for each parameter range (Table 1) and some intermediate values. We use a representative lake surface area of 4,000 km^2, based on observations (Palucis et al.,

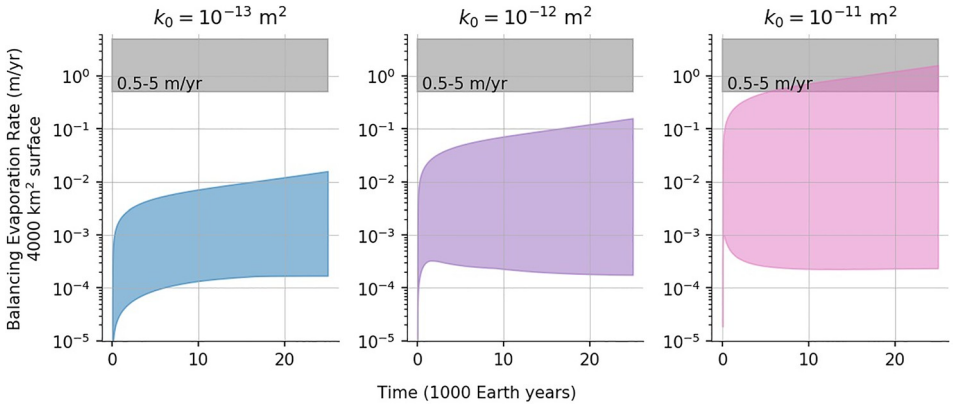

Figure 4. The range of balancing evaporation rates for all model trials over 25,000 yr, grouped by the surface permeability k_0. The balancing evaporation rate is that which closes the water budget of the lake, assuming groundwater is the only input and evaporation is the only outflow. The lowest permeability profile simulated, with $k_0 = 10^{-14}$ m^2, is not shown. The gray box indicates the range 0.5-5 m/yr, discussed in section 5.

2016). The size of the lake is important, however. For example, a lake ten times larger would require ten times as much water to balance evaporation. We discuss this more in the following section.

Figure 4 shows this balancing evaporation rate for all model trials over 25,000 yr, grouped by the surface permeability k_0. The range in each panel mostly represents the difference between maximum recharge and zero recharge. With maximum recharge, the top of each range is proportional to the permeability. With zero recharge, the water table drops over time, decreasing the hydraulic gradient and reducing flow. This feedback occurs faster with increasing permeability, explaining the wide range for $k_0 = 10^{-11}$ m^2.

Figure 5 shows initial and final temperature fields for a simulation with a warmer initial surface temperature of 250 K. After enough time, the crust beneath thawed regions of the surface will thaw through completely, connecting the surface to deep parts of the crust. However, above-freezing surface temperatures in Gale do not necessarily imply the same for adjacent terrain. The assumed lapse rate and surface temperature in Gale control which parts of the surface thaw. For example, warming the surface temperature in the crater only slightly above the freezing point, to 275 K, prevents the surface from thawing anywhere outside the crater because of the increasing elevation. Warming to 285 K thaws the flat area north of the crater for the entire lapse rate range, but the southern highlands remain frozen. Only for the shallowest lapse rate, 2.5 K/km, and a surface temperature in the crater above 290 K, do the highlands thaw at the surface.

5. Discussion

Figure 2 shows that higher thermal conductivity increases the time required to thaw the frozen layer of the crust near the surface. This relationship is driven by the geothermal gradient's dependence on the conductivity. Although higher thermal conductivity leads to faster thawing, it also decreases the geothermal gradient. With a geothermal gradient of Q/α, where Q is the geothermal heat flux and α is the thermal conductivity, the freezing temperature T_f will be at the vertical level z_f defined by

$$z_f = \frac{\alpha}{Q}(T_s - T_f); \tag{5}$$

where T_s is the surface temperature. Additionally, the time required for a thermal pulse at the surface to travel some depth L is approximately $\tau = \rho_r c L^2/\alpha$. Letting $L = z_f$ and plugging equation (5) into this timescale,

$$\tau = \frac{\rho_r c \alpha}{Q^2}(T_s - T_f)^2. \tag{6}$$

Although it may not be intuitive, Equation 6 shows that the thaw time is expected to be proportional to α after accounting for the geothermal gradient's dependence on α. This expectation is in agreement with the results in Figure 2.

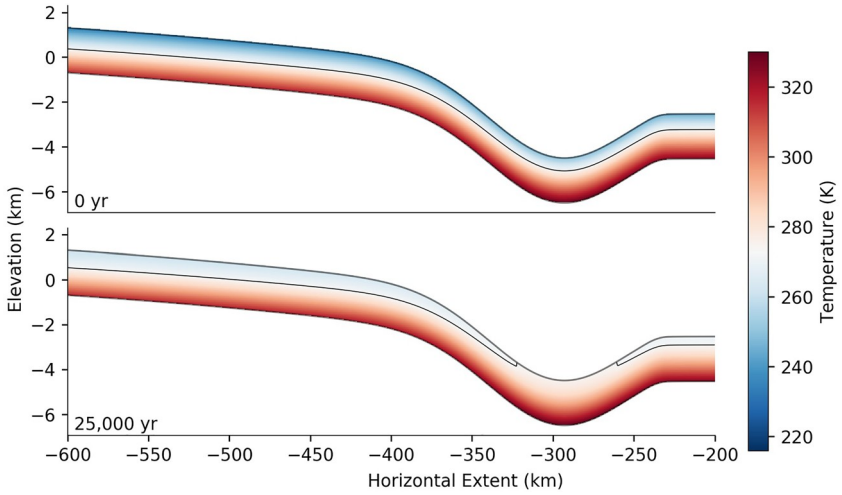

Figure 5. The temperature field in the crust at the beginning and end of a 25,000-yr integration, demonstrating uneven thawing of the crust due to topography. The initial and final surface temperatures in Gale are 250 and 275 K, and α_r = 1 W/m·K. Parts of the domain far from the crater have been cropped (see Figure 1 for the whole domain). There is significant vertical exaggeration. The black line shows the 273 K isotherm.

Groundwater's contribution to the water budget of Gale lakes after rapid warming depends on the rate of evaporation (E) from the lake. Because Gale has no outlet channels, evaporation is the only removal mechanism for lakes in the crater, assuming they did not drain to the subsurface. Accurate prediction for lakes here on Earth is difficult and often requires detailed meteorological data or empirical formulae. In the absence of these tools for early Mars, we use a physically motivated approach to constrain the plausible range of evaporation values.

Palucis et al. (2016) use E= 0.26-3.5 m/yr, based on estimates for present-day Mars, arguing that a warm, thicker atmosphere and a cold, thin one may yield similar evaporation rates because of the opposing effects of pressure and temperature. Although conditions on modern Mars are quite different from those required to fill large lakes, this range appears to be roughly appropriate. On Earth, Friedrich et al. (2018) show that evaporation from Lake Tahoe is about 1 m/yr. Lake Tahoe is a 490 km^2 reservoir in California with a seasonally varying surface temperature of 280-295 K and dry summers. Lake Superior has a colder, more humid climate and loses about 0.6 m/yr to evaporation. Lake Mead, representing an arid Earth climate, loses 2 m/yr. Wordsworth et al. (2015) estimate maximum evaporation, assuming relative humidity of zero, using

$$S_{pot} \sim \frac{C_D |v|}{R_{H_2O} T_a} p_{sat}(T_s); \quad (7)$$

where C_D is a drag coefficient (2.75×10^{-3}), $|v|$ is the wind velocity at a reference height (about 3 m/s), T_a is the atmospheric temperature at that height, R_{H_2O} is the specific gas constant for water, p_{sat} is the saturation vapor pressure from the Clausius-Clayperon relation, and T_s is the surface temperature. Figure 6 shows this potential evaporation for the temperature range 275-295 K, assuming $T_a \approx T_s$. The range is about 1.5-5 m/yr.

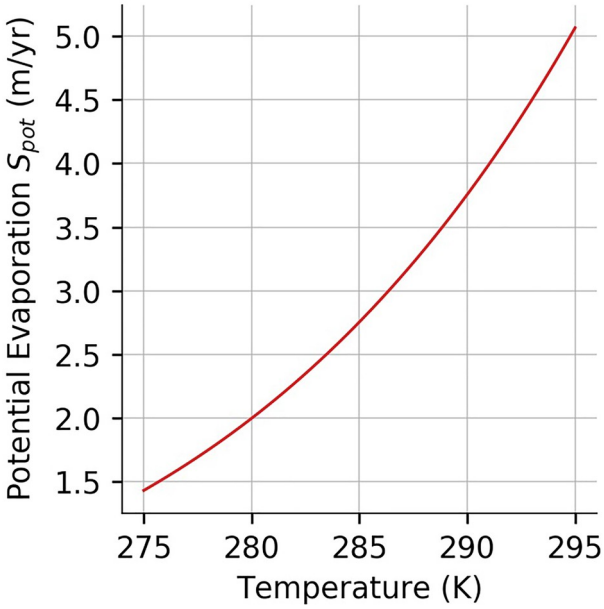

Figure 6. The potential evaporation S_{pot} using $C_D = 2.75 \times 10^{-3}$, $|v|$=3 m/s, and assuming $T_a \approx T_s$.

Collectively, these observations and models of E from large water reservoirs give a range of plausible values for large lakes in Gale of about 0.5-5 m/yr. If temperatures were very low, E could be significantly depressed. However, as discussed in section 4, a denser atmosphere on

early Mars would cause surface temperatures in Gale to be about 15 K warmer than the high-elevation terrain to its south for a lapse rate of 2.5 K/km. If these nearby highlands were warm enough to supply surface water to Gale, as they appear to have been (Palucis et al., 2016), Gale was probably not frozen at the same time. The same reasoning applies to other areas surrounding the crater, although the temperature difference would not have been as large. Seasonal temperature variation also would not dramatically suppress evaporation. Large lakes have high thermal inertia. When lake water temperature lags behind air temperature, evaporation can actually be enhanced during cold, dry winter months.

Given evaporation rates of 0.5-5 m/yr, Figure 4 makes clear that, given 25,000 yr of warmth, groundwater is likely to be a significant source of water to large lakes under only the most favorable conditions considered here. For the highest permeability value, $k_0 = 10^{-11}$ m^2, groundwater delivery equivalent to about 1 m/yr of evaporation from a 4,000 km^2 lake is possible with maximum recharge. This delivery rate exceeds the water required to sustain a lake under low evaporation after a few thousand years. Without high recharge, though, the hydraulic gradient is quickly reduced with high permeability. For $k_0 = 10^{-12}$ m^2, maximum recharge and favorable thermal conditions generate about 0.11 m/yr of evaporative equivalent flow. For $k_0 = 10^{-13}$ m^2 and below, no parameter combinations allow flow above 0.011 m/yr after 25,000 yr. In summary, without high permeability and recharge keeping the water table near the surface, lakes in Gale must be sustained by surface water at the onset of a warm episode.

As mentioned in section 4, the results are dependent on the assumed size of the lake. A surface area of 4,000 km^2 is consistent with analysis of later stage lake deposits (Palucis et al., 2016). However, other lakes may have been different sizes, especially those predating Mount Sharp. The footprint of Mount Sharp is roughly 6,000 km^2 (Deit et al., 2013). Lakes of this size, or larger, would have required even more water input to balance evaporation than lakes with area of 4,000 km^2. If early lakes in Gale covered roughly the area of Mount Sharp, groundwater would have been an even less significant source while the crust was thawing.

Our results are limited to the period before the crust fully thaws beneath Gale. However, we do not assert that lakes or warm periods lasted for no longer than this period. If surface temperatures were warm for long enough to completely thaw the crust, Gale could have been connected to deeper aquifers. This connection could boost groundwater flow and is a natural outcome of long-term, mean surface temperatures above freezing in Gale. For example, Figure 5 shows the temperature evolution of the crust after raising the surface temperature in Gale from 250 to 275 K. The warmer initial temperature causes the crust to thaw through beneath Gale before the end of the simulation. Because the final surface temperature in Gale is only 275 K, the surrounding terrain remains frozen at the surface and only the lower portion of the crater is above freezing. The same pattern could also develop during a cooling phase instead of a warming one, so long as the temperature in Gale is close to the freezing point. If the crust is permeable and saturated beneath the high-elevation permafrost, lakes in Gale could be supplied by deep groundwater. This scenario would be similar to that envisioned by Clifford and Parker (2001), where a subpermafrost aquifer supplies the Martian outflow channels and a northern ocean, but on a smaller scale. S_{pot} is about 1.5 m/yr for 275 K, but with a much larger thickness of crust available for flow and a permeable deeper crust, groundwater might be able to sustain such evaporation. Large, cold, equatorial lakes on Earth could be reasonable analogs if such lakes exist.

6. Conclusion

We have modeled groundwater flow to Gale crater in the first 25,000 yr after surface temperatures transition from cold and frozen to warm and mobile. Our results suggest that for a reasonable range of evaporation rates from closed basin lakes in Gale, groundwater might be an appreciable component of the water budget for large lakes only if the large-scale permeability of the crust is very high and recharge is fast enough to keep the water table near the surface. Without these favorable conditions, surface water must have been the dominant influx at the onset of a warm period.

These results can be compared with prior work assuming the crust is thawed throughout. In their modeling, Horvath and Andrews-Hanna (2017) find subsurface flow accounts for up to 47% of lake influx with a vertically averaged permeability of 3×10^{-13} m^2, a large fraction of the water budget. We suspect the difference is due to the vertically integrated hydraulic permeability and is a meaningful consequence of surface

temperature history. In our modeling and theirs, groundwater flow is governed by the integrated permeability over the layer where groundwater flows. In the warming scenario, however, the mobile region of the crust is only a few hundred meters after 25,000s and a high permeability is required to yield significant groundwater flux. If the crust is fully thawed, the same flux could be achieved by a lower permeability because of the increased depth of flow. This highlights how important the thermal state of the crust may be for lakes in Gale and the relevance of the crust's long thermal time scales.

Our modeling also points toward some consequences of elevation-dependent surface temperatures for Gale hydrology. Because the topography of Gale and its surroundings is so dramatic, surface temperatures in Gale are likely to be about 15 K warmer than in the nearby highlands, on average. This means that if the highlands are warm, Gale is even warmer, promoting evaporation and potentially also precipitation. If, however, average surface temperatures in Gale were near the freezing point, the surrounding terrain would be frozen at the surface. If the crust is permeable at depth, deep aquifers could supply Gale lakes while cool temperatures in the crater depress evaporation. This scenario could help explain the apparent transition from larger lakes sourcing regional water to smaller ones with more local runoff (Palucis et al., 2016), if later episodes left the highlands mostly frozen.

Acknowledgments

The computations in this paper were run on the FASRC Cannon cluster supported by the FAS Division of Science Research Computing Group at Harvard University. Model code is open source and available at Baum (2020b). Supporting code is archived at Baum (2020c). All model results needed to reproduce figures and analysis in this paper are available at Baum (2020a).

References

Batalha, N. E., Kopparapu, R. K., Haqq-Misra, J., & Kasting, J. F. (2016). Climate cycling on early Mars caused by the carbonate-silicate cycle. *Earth and Planetary Science Letters*, *455*, 7-13.

Baum, M. (2020a). Model results for "groundwater flow to Gale Crater in an episodically warm climate". Zenodo, https://doi.org/10.5281/zenodo.3779473

Baum, M. (2020b). wordsworthgroup/bous-therm v1.0.

Baum, M. (2020c). wordsworthgroup/libode v1.0.1.

Bear, J. (1972). *Dynamics of fluids in porous media*. New York: Dover.

Chassefire, E., Lasue, J., Langlais, B., & Quesnel, Y. (2016). Early Mars serpentinization-derived CH4 reservoirs, H2-induced warming and paleopressure evolution. *Meteoritics & Planetary Science*, *51*(11), 2234-2245.

Clifford, S. M. (1993). A model for the hydrologic and climatic behavior of water on Mars. *Journal of Geophysical Research*, *98*(E6),10,973-11,016.

Clifford, S. M., & Parker, T. J. (2001). The evolution of the Martian hydrosphere: Implications for the fate of a primordial ocean and the current state of the northern plains. *Icarus*, *154*(1), 40-79.

Deit, L. L., Hauber, E., Fueten, F., Pondrelli, M., Rossi, A. P., & Jaumann, R. (2013). Sequence of infilling events in Gale Crater, Mars: Results from morphology, stratigraphy, and mineralogy. *Journal of Geophysical Research: Planets*, *118*, 2439-2473. https://doi.org/10.1002/2012JE004322

Demming, D. (2002). *Introduction to hydrogeology*. Boca Raton, FL: McGraw-Hill.

Ehlmann, B. L., & Edwards, C. S. (2014). Mineralogy of the Martian surface. *Annual Review of Earth and Planetary Sciences*, *42*(1), 291-315.

Fassett, C. I., & Head, J. W. (2008). Valley network-fed, open-basin lakes on Mars: Distribution and implications for Noachian surface and subsurface hydrology. *Icarus*, *198*(1), 37-56.

Fedo, C. M., Grotzinger, J. P., Gupta, S., Fraeman, A., Edgar, L., Edgett, K., et al. (2018). Sedimentology and stratigraphy of the Murray formation, Gale Crater, Mars. In *Paper Presented at the 49th Lunar and Planetary Science Conference, 2083*.

Forget, F. (1997). Warming early Mars with carbon dioxide clouds that scatter infrared radiation. *Science*, *278*(5341), 1273-1276.

Forget, F., Wordsworth, R., Millour, E., Madeleine, J.-B., Kerber, L., Leconte, J., et al. (2013). 3D modelling of the early Martian climate under a denser CO_2 atmosphere: Temperatures and CO_2 ice clouds. *Icarus*, *222*(1), 81-99.

Friedrich, K., Grossman, R. L., Huntington, J., Blanken, P. D., Lenters, J., Holman, K. D., et al. (2018). Reservoir evaporation in the western United States: Current science, challenges, and future needs. *Bulletin of the American Meteorological Society*, *99*(1), 167-187.

Frydenvang, J., Gasda, P. J., Hurowitz, J. A., Grotzinger, J. P., Wiens, R. C., Newsom, H. E., et al. (2017). Diagenetic silica enrichment and late-stage groundwater activity in Gale Crater, Mars: Silica enriching diagenesis, Gale, Mars. *Geophysical Research Letters*, *44*, 4716-4724. https://doi.org/10.1002/2017GL073323

Fukushi, K., Sekine, Y., Sakuma, H., Morida, K., & Wordsworth, R. (2019). Semiarid climate and hyposaline lake on early Mars inferred from reconstructed water chemistry at Gale. *Nature Communications*, *10*(1), 4896.

Grotzinger, J. P., Gupta, S., Malin, M. C., Rubin, D. M., Schieber, J., Siebach, K., et al. (2015). Deposition, exhumation, and paleoclimate of an ancient lake deposit, Gale crater, Mars. *Science*, *350*(6257), aac7575.

Grotzinger, J. P., Sumner, D. Y., Kah, L. C., Stack, K., Gupta, S., Edgar, L., et al. (2014). A habitable fluvio-lacustrine environment at Yellowknife Bay, Gale Crater, Mars. *Science*, *343*(6169), 1242777.

Haberle, R. M., Clancy, R. T., Forget, F., Smith, M. D., & Zurek, R. W. (Eds.) (2017). *The atmosphere and climate of Mars*. Cambridge: Cambridge University Press.

Haberle, R. M., Zahnle, K., Barlow, N. G., & Steakley, K. E. (2019). Impact degassing of H2 on early Mars and its effect on the climate system. *Geophysical Research Letters*, *46*, 13,355-13,362. https://doi.org/10.1029/2019GL084733

Halevy, I., & Head, J. W. III. (2014). Episodic warming of early Mars by punctuated volcanism. *Nature Geoscience*, *7*(12), 865-868.

Halevy, I., Zuber, M. T., & Schrag, D. P. (2007). A sulfur dioxide climate feedback on early Mars. *Science*, *318*(5858), 1903-1907.

Hanna, J. C. (2005). Hydrological modeling of the Martian crust with application to the pressurization of aquifers. *Journal of Geophysical Research*, *110*, E01004. https://doi.org/10.1029/2004JE002330

Hauck, S. A. (2002). Thermal and crustal evolution of Mars. *Journal of Geophysical Research*, *107*(E7), 5052. https://doi.org/10.1029/2001JE001801

Hayworth, B. P. C., Kopparapu, R. K., Haqq-Misra, J., Batalha, N. E., Payne, R. C., Foley, B. J., et al. (2020). Warming early Mars with climate cycling: The effect of CO_2-H_2 collision-induced absorption. *Icarus*, *345*, 113,770.

Horvath, D. G., & Andrews-Hanna, J. C. (2017). Reconstructing the past climate at Gale crater, Mars, from hydrological modeling of late-stage lakes: Lake hydrology at Gale Crater. *Geophysical Research Letters*, *44*, 8196-8204. https://doi.org/10.1002/2017GL074654

Hu, H., & Argyropoulos, S. A. (1996). Mathematical modelling of solidification and melting: A review. *Modelling and Simulation in Materials Science and Engineering*, *4*(4), 371.

Hurowitz, J. A., Grotzinger, J. P., Fischer, W. W., McLennan, S. M., Milliken, R. E., Stein, N., et al. (2017). Redox stratification of an ancient lake in Gale crater, Mars. *Science*, *356*(6341), eaah6849.

Hynek, B. M., Beach, M., & Hoke, M. R. T. (2010). Updated global map of Martian valley networks and implications for climate and hydrologic processes. *Journal of Geophysical Research*, *115*, E09008. https://doi.org/10.1029/2009JE003548

Kasting, J. F. (1991). CO2 condensation and the climate of early Mars. *Icarus*, *94*, 1-13.

Kerber, L., Forget, F., & Wordsworth, R. (2015). Sulfur in the early Martian atmosphere revisited: Experiments with a 3-D Global Climate Model. *Icarus*, *261*, 133-148.

Palucis, M. C., Dietrich, W. E., Williams, R. M. E., Hayes, A. G., Parker, T., Sumner, D. Y., et al. (2016). Sequence and relative timing of large lakes in Gale crater (Mars) after the formation of Mount Sharp. *Journal of Geophysical Research: Planets*, *121*, 472-496. https://doi.org/10.1002/2015JE004905

Palumbo, A. M., Head, J. W., & Wordsworth, R. D. (2018). Late Noachian Icy Highlands climate model: Exploring the possibility of transient melting and fluvial/lacustrine activity through peak annual and seasonal temperatures. *Icarus*, *300*, 261-286.

Rae, A. S. P., Collins, G. S., Morgan, J. V., Salge, T., Christeson, G. L., Leung, J., et al. (2019). Impact-induced porosity and microfracturing at the Chicxulub impact structure. *Journal of Geophysical Research: Planets*, *124*, 1960-1978. https://doi.org/10.1029/2019JE005929

Ramirez, R. M., & Craddock, R. A. (2018). The geological and climatological case for a warmer and wetter early Mars. *Nature Geoscience*, *11*(4), 230-237.

Ramirez, R. M., Kopparapu, R., Zugger, M. E., Robinson, T. D., Freedman, R., & Kasting, J. F. (2014). Warming early Mars with CO_2 and H_2. *Nature Geoscience*, *7*(1), 59-63.

Rampe, E. B., Ming, D. W., Blake, D. F., Bristow, T. F., Chipera, S. J., Grotzinger, J. P., et al. (2017). Mineralogy of an ancient lacustrine mudstone succession from the Murray formation, Gale crater, Mars. *Earth and Planetary Science Letters*, *471*, 172-185.

Rapin, W. (2019). An interval of high salinity in ancient Gale crater lake on Mars. *Nature Geoscience*, *12*, 889-895.

Sagan, C. (1977). Reducing greenhouses and the temperature history of Earth and Mars. *Nature*, *269*(5625), 224-226.

Segura, T. L. (2002). Environmental effects of large impacts on Mars. *Science*, *298*(5600), 1977-1980.

Siebach, K. L., & Grotzinger, J. P. (2014). Volumetric estimates of ancient water on Mount Sharp based on boxwork deposits, Gale Crater, Mars: Boxwork deposits on Mount Sharp. *Journal of Geophysical Research*, *119*, 189-198. https://doi.org/10.1002/2013JE004508

Stack, K. M., Grotzinger, J. P., Lamb, M. P., Gupta, S., Rubin, D. M., Kah, L. C., et al. (2019). Evidence for plunging river plume deposits in the Pahrump Hills member of the Murray formation, Gale crater, Mars. *Sedimentology*, *66*(5), 1768-1802.

Steakley, K., Murphy, J., Kahre, M., Haberle, R., & Kling, A. (2019). Testing the impact heating hypothesis for early Mars with a 3-D global climate model. *Icarus*, *330*, 169-188.

Stein, N., Grotzinger, J. P., Schieber, J., Mangold, N., Hallet, B., Newsom, H., et al. (2018). Desiccation cracks provide evidence of lake drying on Mars, Sutton Island member, Murray formation, Gale Crater. *Geology*, *46*(6), 515-518.

Thomas, N. H., Ehlmann, B. L., Meslin, P. Y., Rapin, W., Anderson, D. E., Rivera Hernndez, F., et al. (2019). Mars science laboratory observations of chloride salts in Gale crater, Mars. *Geophysical Research Letters*, *46*, 10,754-10,763. https://doi.org/10.1029/2019GL082764

Urata, R. A., & Toon, O. B. (2013). Simulations of the Martian hydrologic cycle with a general circulation model: Implications for the ancient Martian climate. *Icarus*, *226*(1), 229-250.

Williams, R. M. E., Grotzinger, J. P., Dietrich, W. E., Gupta, S., Sumner, D. Y., Wiens, R. C., et al. (2013). Martian fluvial conglomerates at Gale crater. *Science*, *340*(6136), 1068-1072.

Wordsworth, R. (2016). The climate of early Mars. *Annual Review of Earth and Planetary Sciences*, *44*(1), 381-408.

Wordsworth, R., Forget, F., & Eymet, V. (2010). Infrared collision-induced and far-line absorption in dense CO_2 atmospheres. *Icarus*, *210*(2), 992-997.

Wordsworth, R., Forget, F., Millour, E., Head, J. W., Madeleine, J.-B., & Charnay, B. (2013). Global modelling of the early Martian climate under a denser CO_2 atmosphere: Water cycle and ice evolution. *Icarus*, *222*(1), 1-19.

Wordsworth, R., Kalugina, Y., Lokshtanov, S., Vigasin, A., Ehlmann, B., Head, J., et al. (2017). Transient reducing greenhouse warming on early Mars. *Geophysical Research Letters*, *44*, 665-671. https://doi.org/10.1002/2016GL071766

Wordsworth, R., Kerber, L., Pierrehumbert, R. T., Forget, F., & Head, J. W. (2015). Comparison of "warm and wet" and "cold and icy" scenarios for early Mars in a 3-D climate model. *Journal of Geophysical Research: Planets*, *120*, 1201-1219. https://doi.org/10.1002/2015JE004787

Wordsworth, R., & Pierrehumbert, R. (2013). Hydrogen-nitrogen greenhouse warming in the Earth's early atmosphere. *Science*, *339*, 64-67.

Yen, A. S., Ming, D. W., Vaniman, D. T., Gellert, R., Blake, D. F., Morris, R. V., et al. (2017). Multiple stages of aqueous alteration along fractures in mudstone and sandstone strata in Gale Crater, Mars. *Earth and Planetary Science Letters*, *471*, 186-198.